Spectroscopic Investigation of Laser Energy Deposition in Low-Density Foams

O. Renner,[1] J. Limpouch[2], E. Krousky[1], O. Klimo[2], D. Klir[2], R. Liska[2], W. Nazarov[3], N.G. Borisenko[4], J. Ullschmied[5]

[1]Institute of Physics, Academy of Sciences CR, Prague, Czech Republic
[2]Czech Technical University in Prague, Faculty of Nuclear Sciences, Czech Republic
[3]University of St. Andrews, School of Chemistry, St. Andrews, UK
[4]P.N. Lebedev Physical Institute of RAS, Moscow, Russia
[5]Institute of Plasma Physics, Academy of Sciences CR, Prague, Czech Republic

3rd Moscow Workshop on Targets and Applications, Moscow, October 15 - 19, 2007

Syllabus:

- Motivation for investigation of laser energy deposition in low-density foams
- Laser-foam interaction, survey of previous spectral studies
- Spectroscopic experiments at PALS
- Results, interpretation of high-resolution x-ray spectra
- Selected prospective applications
- Conclusions

Acknowledgments

This research was performed at the Prague Asterix Laser Facility and supported by Czech Science Foundation under grant No. 202/06/0801.

Research Motivation

Laser energy deposition & radiative properties of underdense targets:

- **low-density porous materials (closed, semi-closed or open cells)**
- **electron content ≤ critical laser density $n_c = 1.12\times10^{21}/(\lambda[\mu m])^2$**

Applications of foams in laser-matter interactions

- **ablation pressure smoothing in direct-drive ICF targets**
- **dynamic phase plate for laser beam homogenization**
- **efficiency enhancement of ion acceleration by fs pulses conversion to x rays (backlighters)**
- **atomic physics studies (non-LTE systems, radiative transport, intensifying the shock wave pressure for EOS studies)**
- **astrophysically related experiments**

Highlights of reported x-ray spectroscopic experiments:

- **narrow-band absolute radiance of Cl-doped foams**
- **environmental parameters in laser-irradiated foams**
- **experimental feedback for development of theoretical models**

Laser-Foam Interaction

Underdense foams vs. standard-density solid materials:

laser penetration depth >> λ_{laser} (fraction of λ_{laser} in foils)

Generally accepted energy deposition mechanism:
fast partial ionization by multiphoton processes
rest of laser energy absorbed by inverse bremsstrahlung →
ionization wave outruns hydrodynamic perturbations →
volumetrically heated plasma, little energy lost in hydromotion
cell walls expand and fill the pores (fast homogenization stage)
collision of mass fluxes, inhomogeneities damped out by viscosity (slow homogenization stage)

Survey of previous studies:

Koch J.A. et al, Phys. Plasmas 2 (1995) 3280
Fournier K.B. et al, PRL 92 (2004) 165005
Limpouch J. et al, Plasma Phys. Control. Fusion 46 (2004) 1831
Back C.A. et al, JQSRT 99 (2006) 21

Interaction Experiments at Prague Asterix Laser System

Research goals:

- **Laser absorption & energy transport in directly heated foams**
- **Shock wave propagation**
- **Transmission through foams**
- **Diagnosis of volumetric plasma**
- **Hi-res x-ray spectroscopy at medium-Z doped plastic foams**
- **Collection of precise data – benchmark for simulations**

PALS - iodine photodissociation high-power laser system
single Gaussian-profile beam (1000 J/1ω, 1.315 μm, 0.3 ns, 80 μm, 7×10^{16} Wcm^{-2})
frequency-tripled radiation (300 J/3ω, 0.44 μm, pulse length 0.25-0.3 ns)

Jungwirth K. et al, Phys. Plasmas 8 (2001) 2495

Spectroscopic Experiment: Diagnostic Complex & Targets

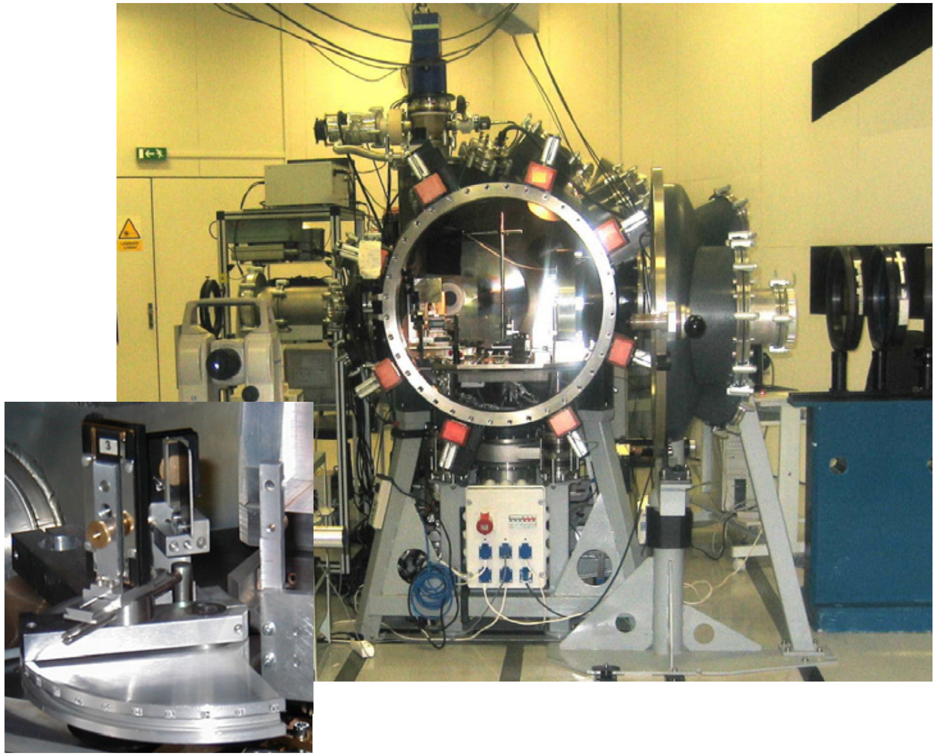

Principal diagnostics:
x-ray vertical dispersion
Johann spectrometer (VJS)

Complementary diagnostics:
calorimeter + opt. streak camera
(laser light transmission
through foam layers)
filtered pinhole + CCD imaging
(x-ray emitting surface area)
slit + x-ray streak camera
(heat front propagation)

Targets: Cl-doped TMPTA (trimethylolpropane triacrylate, $C_{15}H_{20}O_6$) foams
monomer dissolved and photo-initiated, free radical polymerization
produced gel precipitated in a non-solvent, subsequent super critical drying
foam densities [mg/cm^3]/weight % of chlorine: 10/20, 20/10, 20/20

Nazarov W. et al, Fusion Sci. Technol. 41 (2002) 193; J. Mat. Sci. 41 (2006) 3973

Supporting Diagnostics: Pinhole Foam Surface Imaging

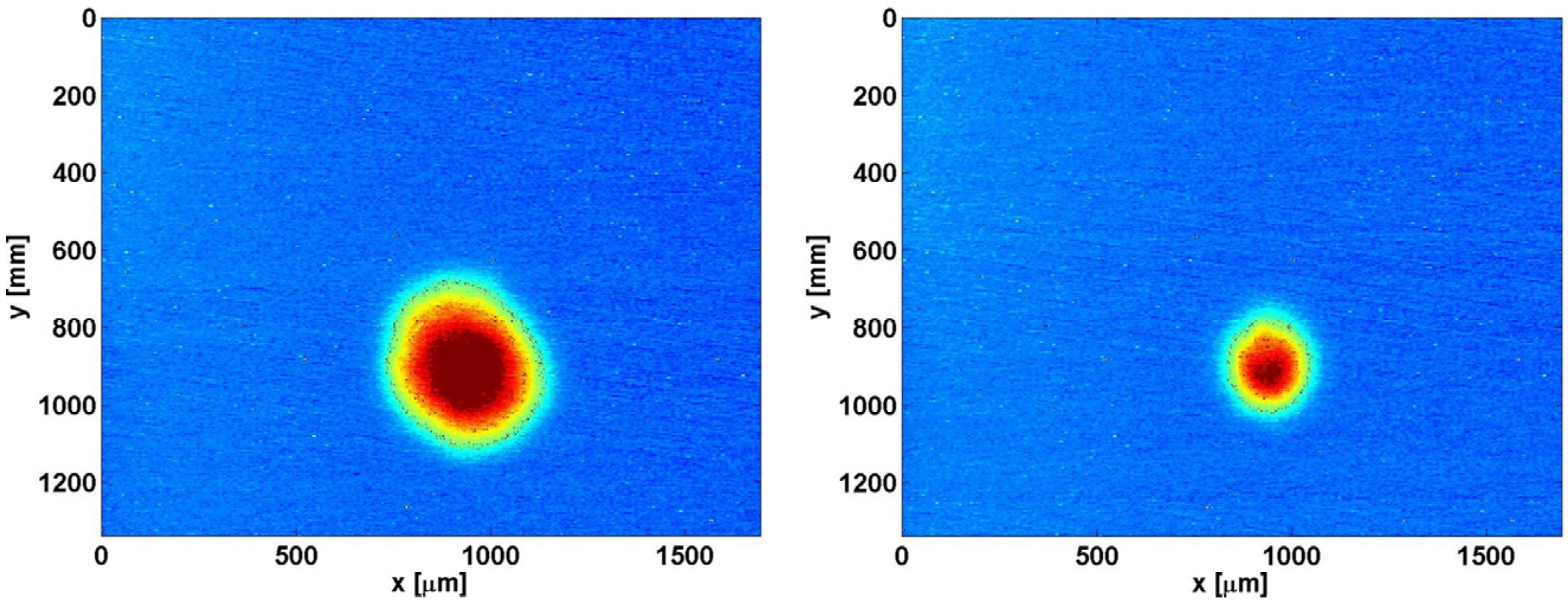

Filtered pinhole images (photon energy > 1.5 keV)

left – foam surface 500 µm behind the best laser-light focus: laser spot ø 250 µm, x-ray emitting region ø 290 µm

right – best focus on surface: laser spot ø 80 µm, x-ray ø 160 µm

tight focus – x-ray radiance of volumetrically heated plasma is higher but due to smaller emitting volume, the overall emission is practically constant

Supporting Diagnostics: Side-on Streaked X-Ray Images

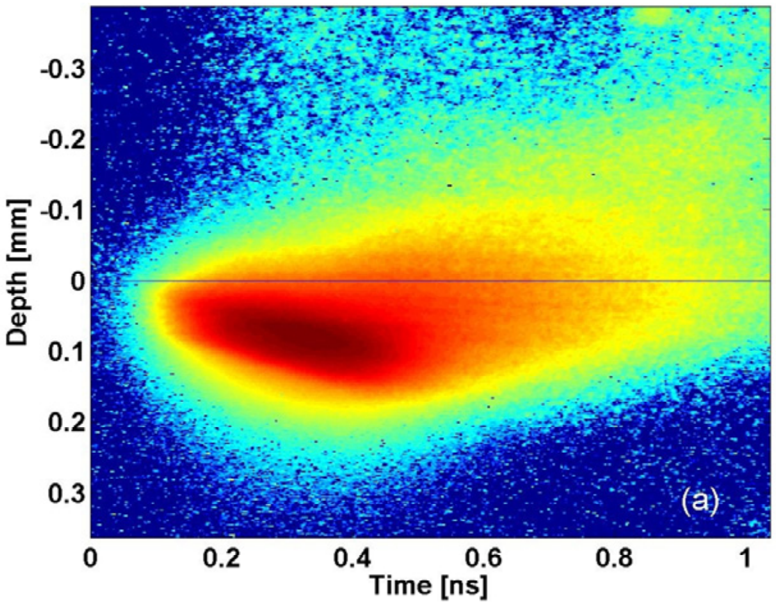

10/20 foam ($C_{15}H_{20}O_6Cl_{2.1}$, $n_{e,tot} \approx 0.54\ n_c$)

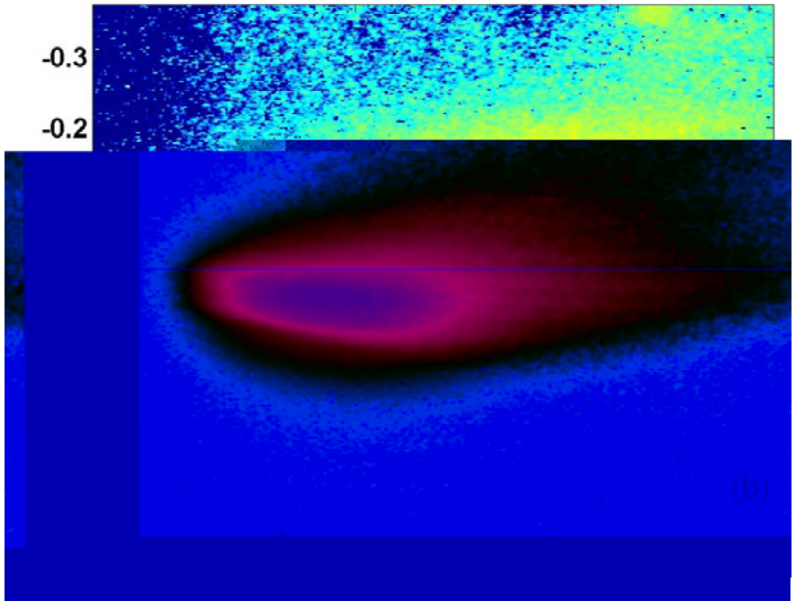

20/10 foam ($C_{15}H_{20}O_6Cl_{0.93}$, $n_{e,tot} \approx 1.1\ n_c$)

x-ray streak camera logarithmic signal (effective photon energy > 1 keV),
laser spot ø 250 µm, laser energy 160 J
in underdense foam (a), hot plasma layer emitting hard x rays is thicker,
the ionization wave propagates deeper and slightly faster
as compared to overdense foam (b)

Vertical-Geometry Johann Spectrometer

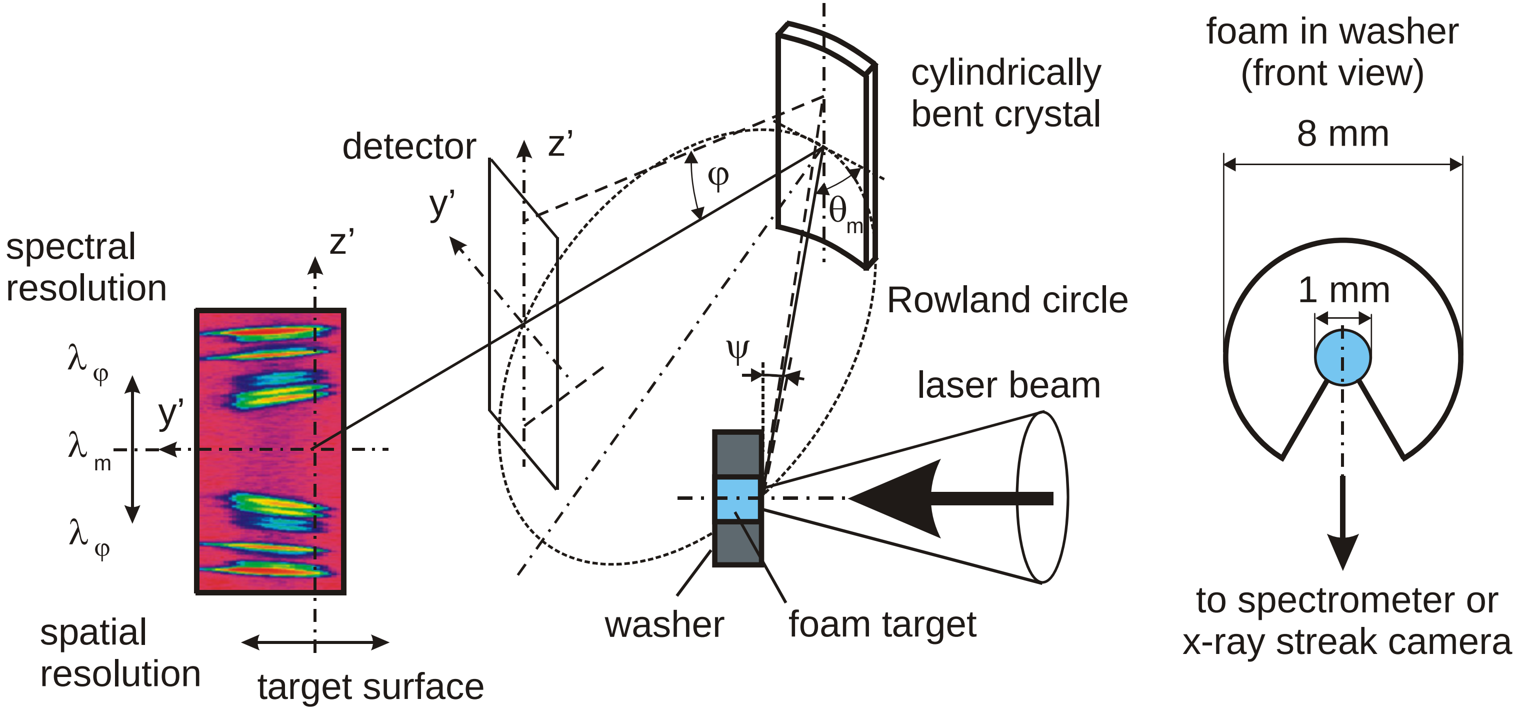

Characteristics: **spectra dispersed as a function of φ:** $\lambda = \lambda_o \cos\varphi$

Cl Heα (4.444 Å) and Lyα (4.185 Å) at $\psi = 2 \pm 0.8^o$ to foam surface

quartz (110), R = 76.6 mm, spectral resolution >5000, spatial 8 µm

linear dispersion ~190 mm/Å, wavelength coverage 2x100 mÅ

single shot spectra, x-ray film Kodak Industrex CX

*Renner O. et al, RSI **68** (1997) 2393*

Evaluation of the Observed Spectra

Computerized reconstruction of the raw high-resolution and high-dispersion spectral data based on previously published algorithms

*Renner O. et al, RSI **68** (1997) 2393*

Decomposition of the complex spectra into individual line components, detailed line identification

Peak Fitting Module, http://www.astonsci.co.uk/assets/files/originpro75

Adámek P. et al, LPB 24 (2006) 511

Estimation of the macroscopic plasma parameters using diagnostic codes FLY and FLYCHK

Lee R.W. et al, JQSRT 56 (1996) 535

Chung H.K. et al, High Energy Density Physics 1 (2005) 3

Comparison of the found plasma characteristics with predictions of 1D and 2D hydrodynamic simulations

Kucharik M. et al, J. Phys. IV France 133 (2006) 167

Liska R. et al, Proc. IFSA (2007), in print

Reconstructed Spectra of Cl Heα and Lyα Group

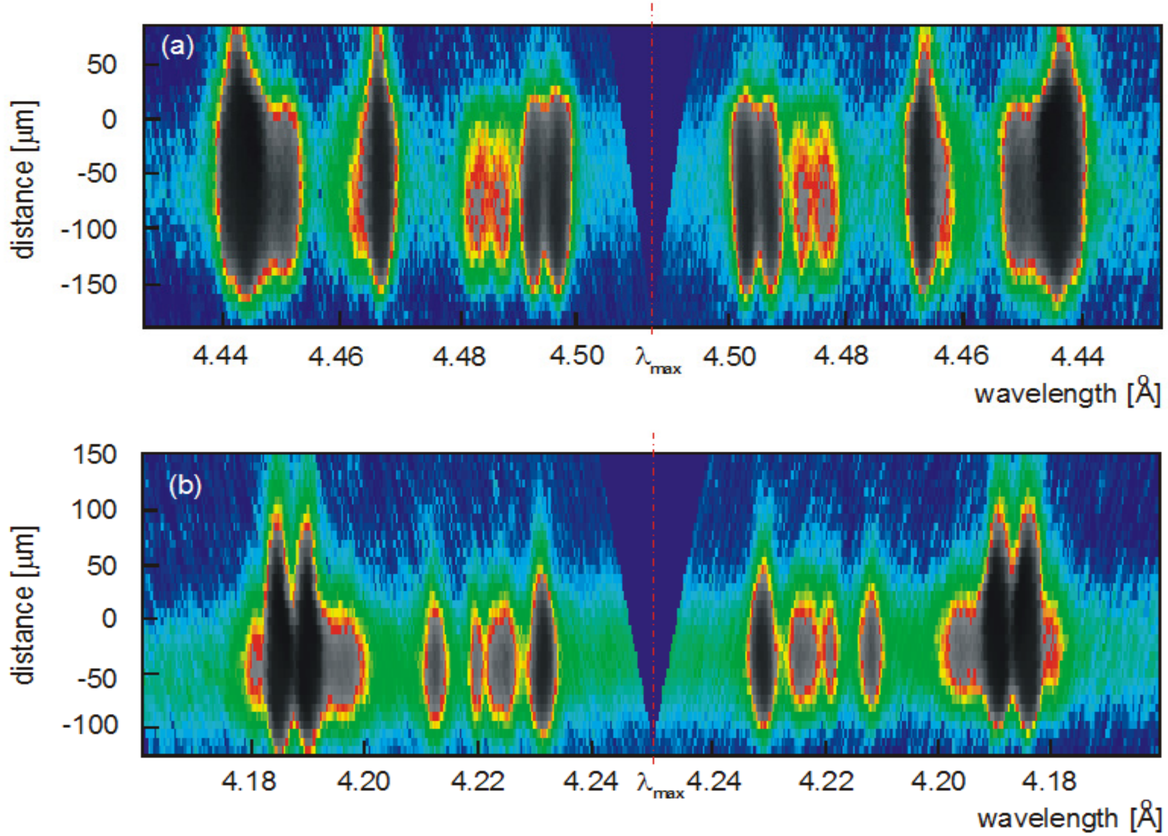

TMPTA Cl-doped foam (10 mg/cm^3, 20 weight % of Cl), thickness 480 µm
laser energy (a) 128 J (b) 151 J/3ω (0.44 µm), pulse length 0.3 ns,
focal spot ø 250 µm (500 µm above the irradiated target surface)

Characteristic Features of the Observed Line Emission

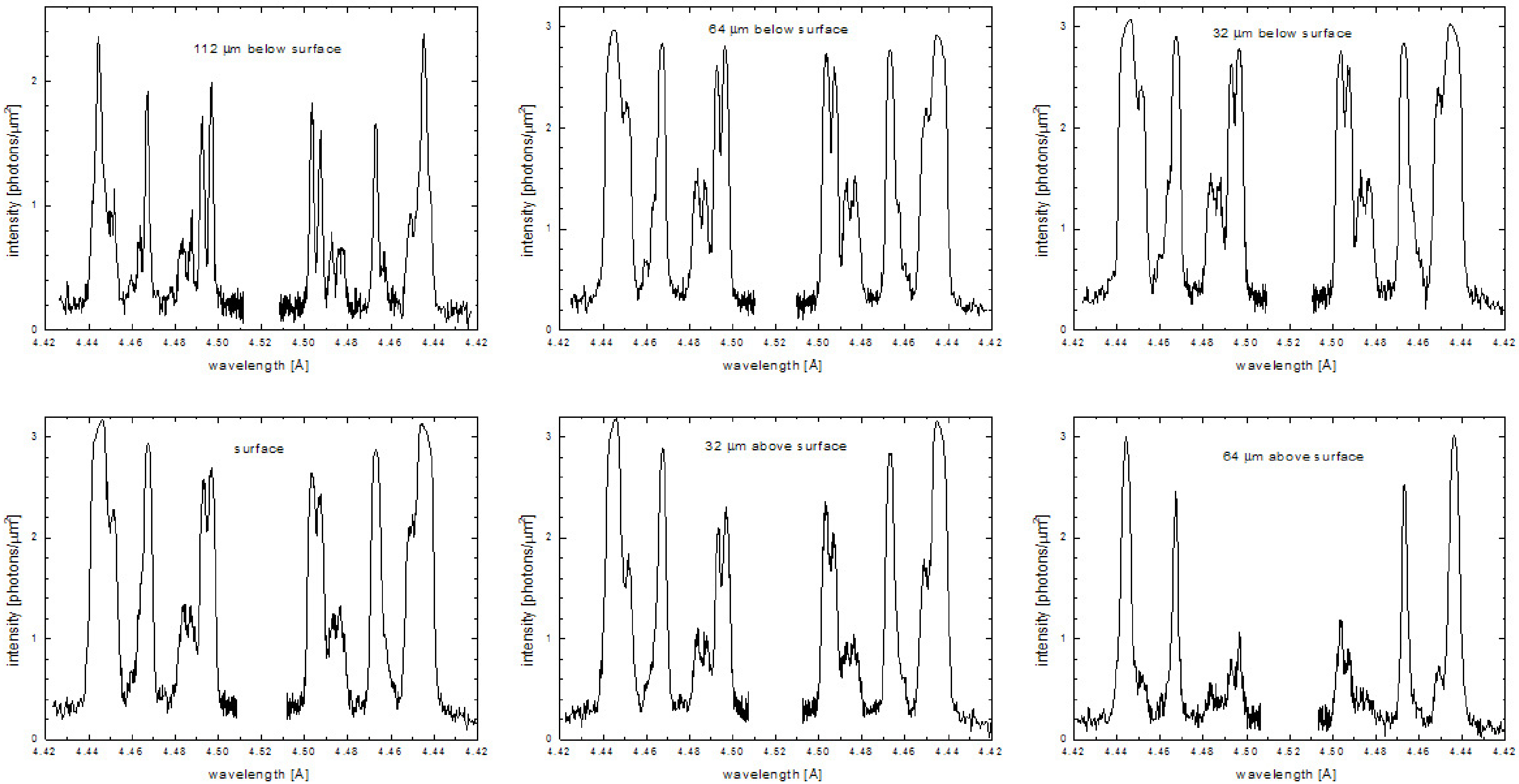

Cl Heα group, TMPTA Cl-doped foam (10 mg/cm³, 20 weight % of Cl)
non-variable satellite structure until ~100 µm below original foam surface

Spectra Decomposition: Genetic Algorithm Approach

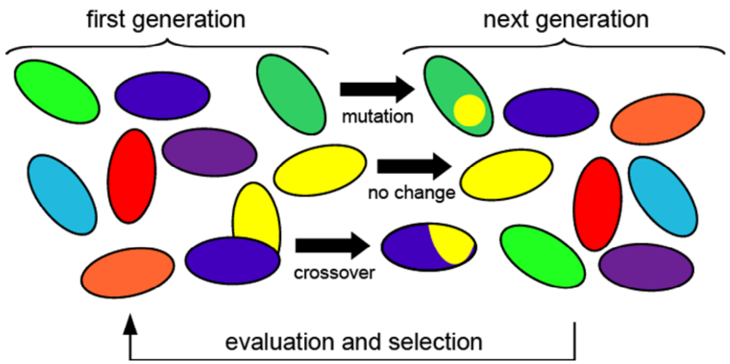

Genetic Algorithm for Spectral Decomposition
set of genomes (trial solutions) → population
population in given GA step → generation
basic operators: crossover, mutation, selection
search space explored, solution quality grows

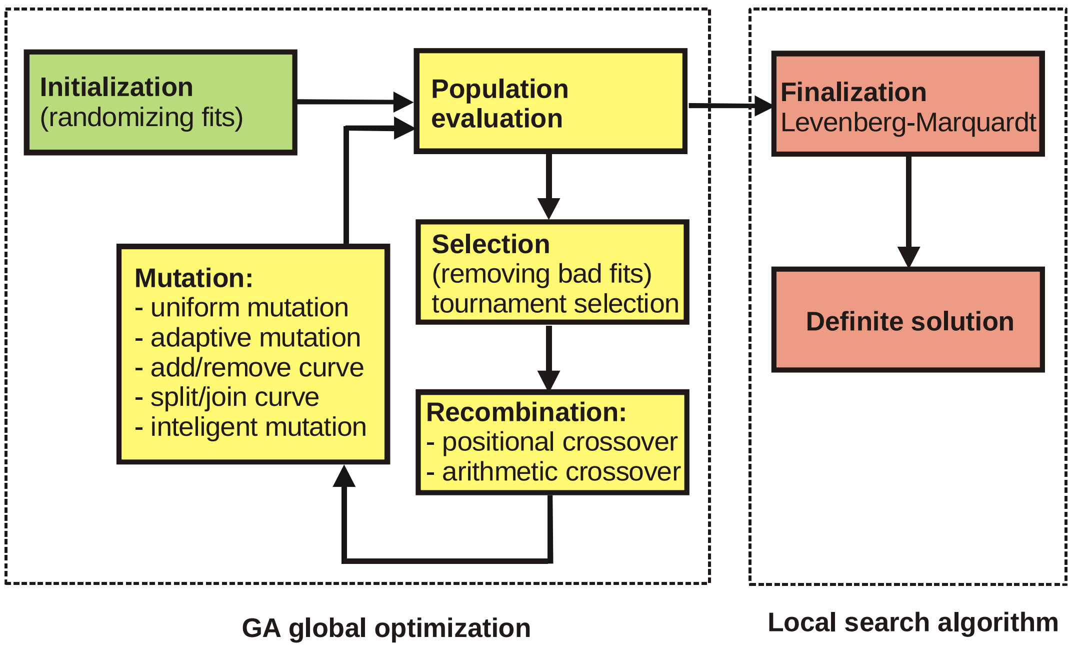

GASPED characteristics:

- pseudo-Voigt line profiles
- genome size: 26-38 parameters
- population: 250 - 500 genomes
- 8 operators tailored to a problem of spectral decomposition
- number of generations ~ 1000
- final fit refined by L-M method

Adámek P. et al, LPB 24 (2006) 511

GA Based Analysis of Cl Heα and Lyα Spectra

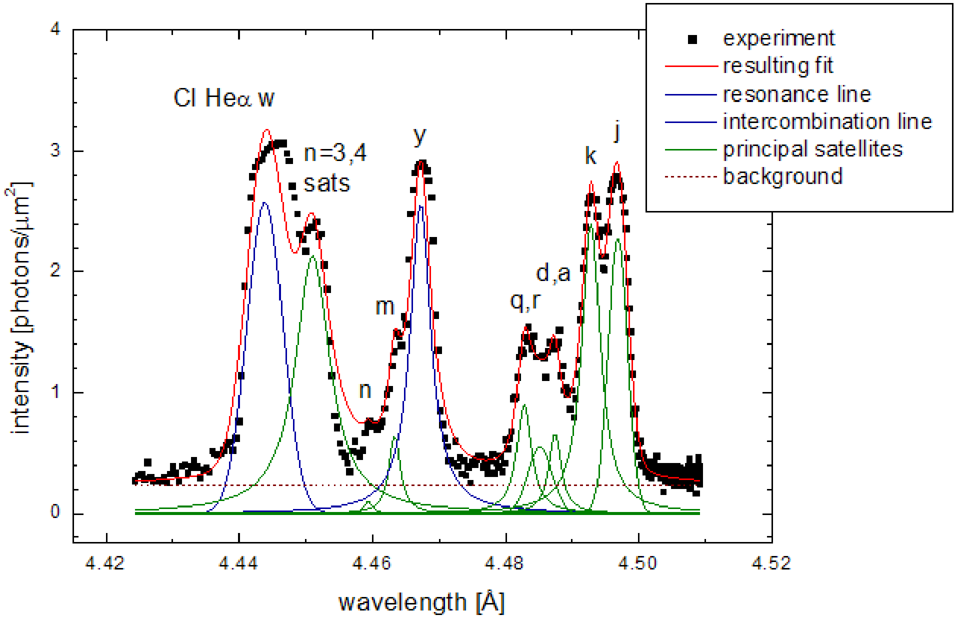

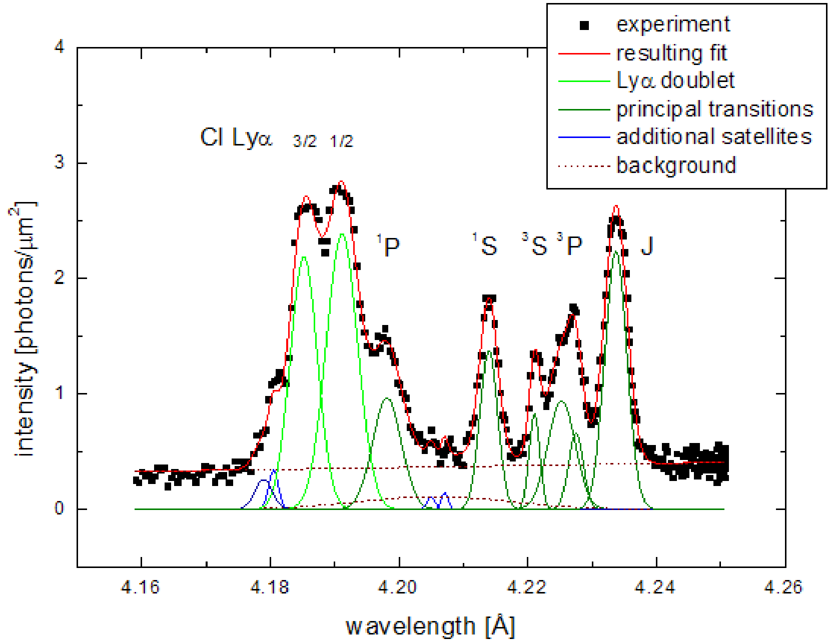

Both spectra correspond to a distance 32 μm below the irradiated foam surface
spectral line identification in Heα group uses Gabriel's notation
satellites to Lyα doublet grouped according to final transition states

Renner O. et al, JQSRT 71 (2001) 623

GASPED derived intensities of individual spectral components provide input for the opacity-corrected version of the code FLY *Lee R.W. et al, JQSRT 56 (1996) 535*

Radiance of Volumetricaly Heated Foams

Radiance of homogeneously emitting foam volumes in spectral lines was derived using the transfer function of the absolutely calibrated VJS hitherto processed results demonstrate the relevance of three investigated factors for source radiance S_r [ph/(µm^2 mrad^2)]:

S_r vs. laser pulse energy (Cl Heα emission, foam 10/20, position -500 µm):

laser energy [J]	60	128	212
S_r	42	82	246

S_r vs. target position (- value: the best focus above the 10/20 foam surface):

position [µm]	-500	0	+500
S_r (at ~130 J)	82	180*	85**

*emitting volume smaller, integrated source emission is practically constant

**volume larger by a factor of 1.4, integrated source emission 1.5× higher

S_r vs. foam type (target position -500, laser energy ~130 J):

foam type	10/20	20/10	20/20
S_r	82	68	85

Cl Lyα emission (foam 10/20, position -500 µm, 151 J):

S_r = 31 ph/(µm^2 mrad^2)

Selected Macroscopic Characteristics of Heated Foams

Integrated volumetrically heated source emission (foam 10/20, focus -500):

Cl Heα res. line (E=2790 eV, ΔE=12.9 eV) **1.1×10^{-2} J/4π (2.58×10^{13} photons/4π)**

Cl Lyα doublet (E=2960 eV, ΔE=10.6 eV) **4.7×10^{-3} J/4π (9.90×10^{12} photons/4π)**

Laser light conversion efficiency into full Heα group: 0.02%

cf. reported 2% laser light conversion efficiency into x-ray broadband radiation 4.5-5.5 keV (3 mg/3% Ti-doped SiO_2 aerogel, 40 beams, 3-15 000 J, OMEGA laser, Rochester)

Constantin C. et al, Phys. Plasmas 12 (2005) 063104

Depth of the homogenously emitting plasma

varied in dependence on the focal position:

at 130 J, from 96 µm (target position -500) via 120 µm (0) to 136 µm(+500),

and increased with the laser energy (from 56 to 104 µm)

dependences on foam density were not decisive:

at low energies, penetration was largest for thinnest foam 10/20 (96 µm)

practically constant for high energies (88-104 µm)

Electron Temperature and Density

parameters corresponding to homogeneously emitting plasmas
were determined from opacity-corrected version of the code FLY
Lee R.W. et al, JQSRT 56 (1996) 535

resonance lines were found to be optically thick even in low-density foams
(optical depths ~100 and ~10 for He and Lyα, respectively)
hence the method of isocontour intersections providing couples of (T_e, n_e)
for experimentally determined ratios of optically thin
intercombination and satellite lines was applied

effective values of n_e were consistent with the electron content in foams
(2-3 and 5-6×10^{21} cm^{-3})

effective T_e determined from individual spectral components in Cl Heα group
varied within 520-670 eV (±20 eV)
T_e ~400 eV was found from the ratios of Lyα satellites (jkl/J → $T_e \geq$1000 eV)
univocal trends in electron temperature have not been observed,
interpretation of plasma parameters requires a more detailed atomic code

2D Simulation of Plasma Dynamics: PALE Code

Prague Arbitrary Lagrangian-Eulerian Code (PALE) is substantially Lagrangian code where the mesh rezoning and conservative remapping of physical quantities (Eulerian part) is used to eliminate distortion of Lagrangian cells

PALE is one-fluid code using QEOS or ideal gas + ionization, laser propagation via ray tracing including collisional absorption in underdense plasma and/or absorption at critical surface, Spitzer-Harm heat conductivity with flux limiter

Liska R. et al, J. Phys. IV 133 (2006) 167

foam is modeled by a sequence of different-size pores combining dense slabs with density 0.1 g/cm^3 separated by voids with density 1 mg/cm^3 or, alternatively, by the uniform density material

full thickness of the foam target was 480 μm, prospective absorption at the critical surface was estimated from 1D simulations

Liska R. et al, 5th IFSA Conf., Kobe, Japan (2007), in print

Temperature Evolution in TMPTA Foam

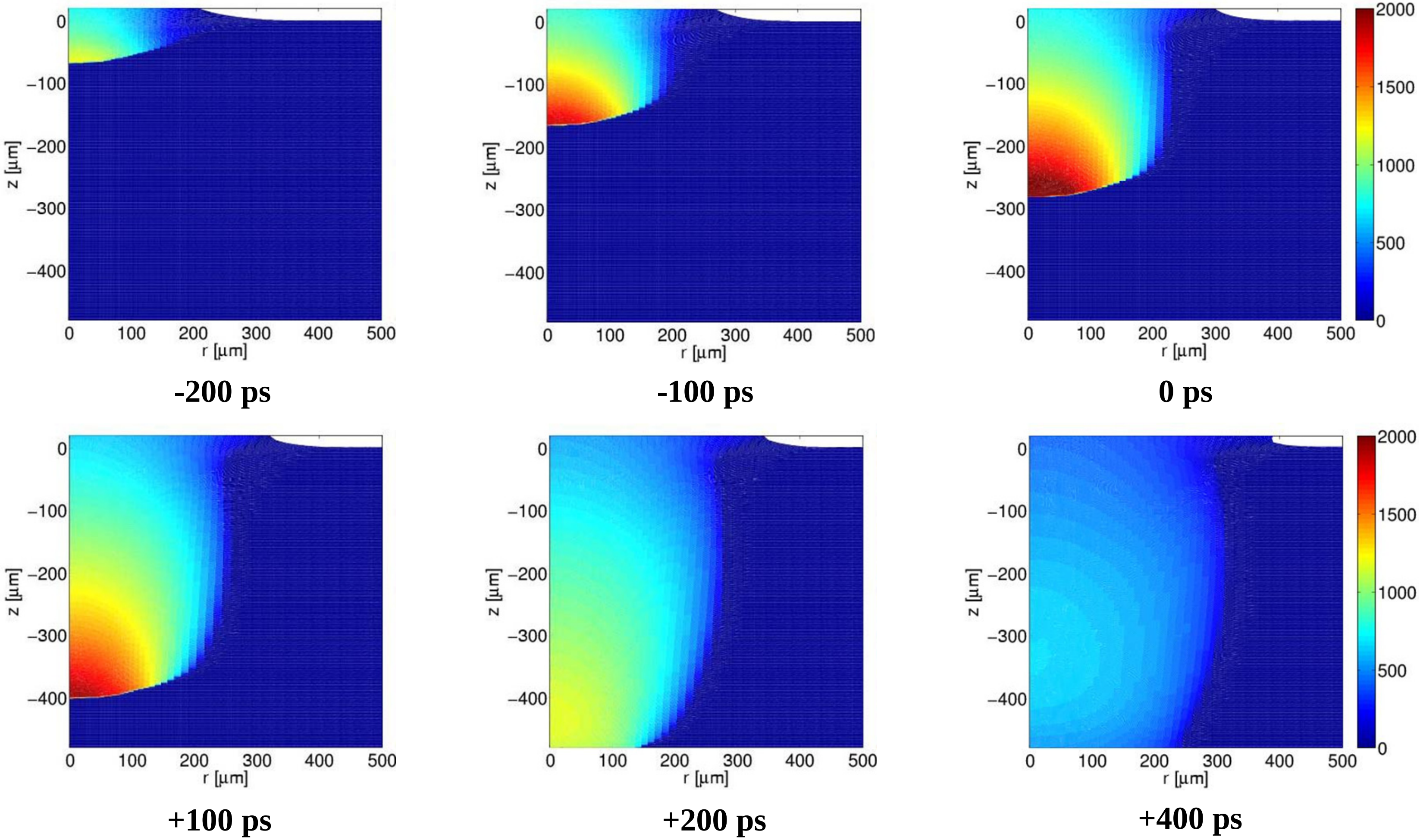

Structured foam, density 10 mg/cm³, pore size 2 µm, foam thickness 480 µm

Simulations for Structured & Uniform Density Foam

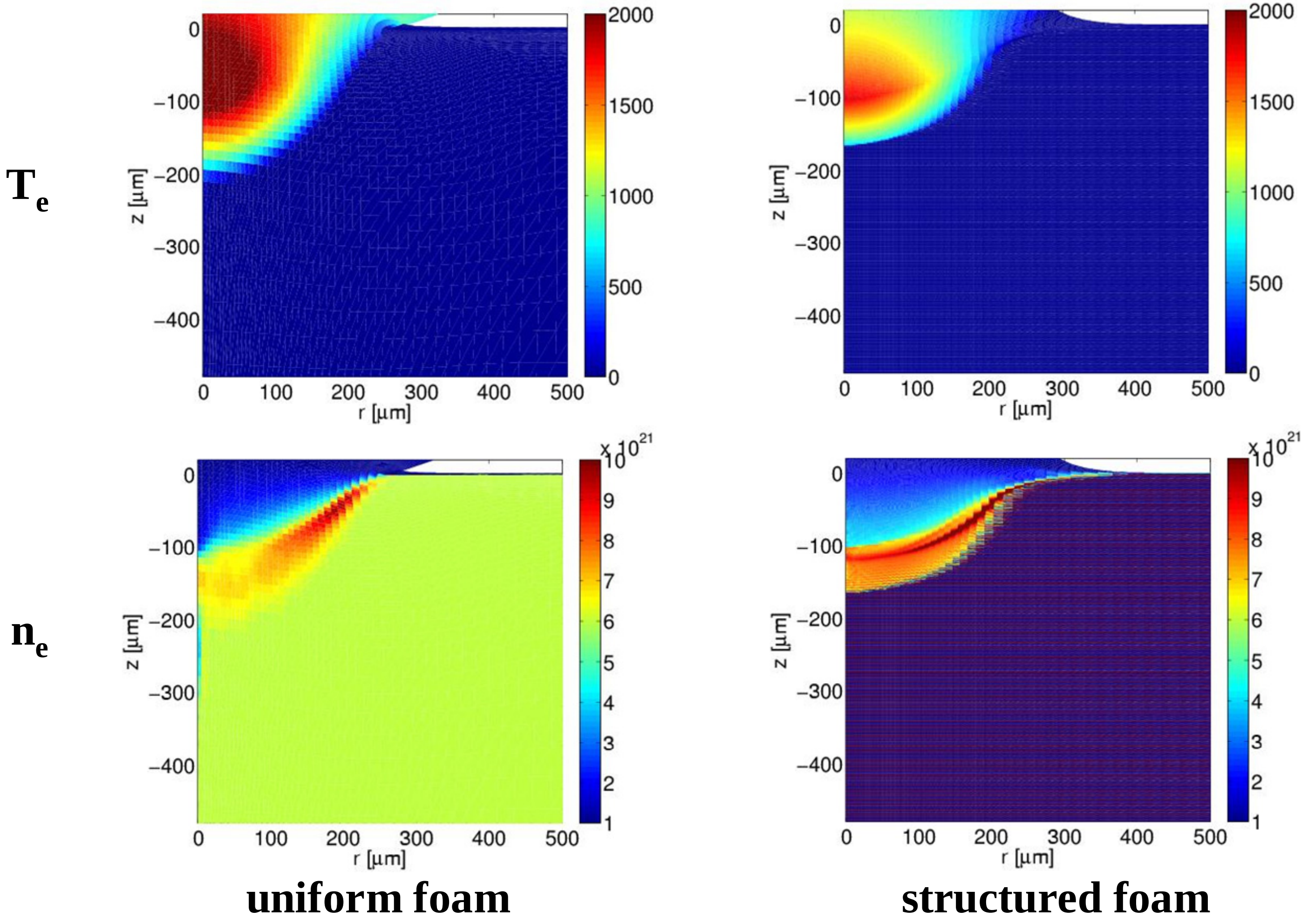

TMPTA foam, density 20 mg/cm³, foam thickness 480 µm, 0 ps

Prospective Applications: Radiative Transfer Effects

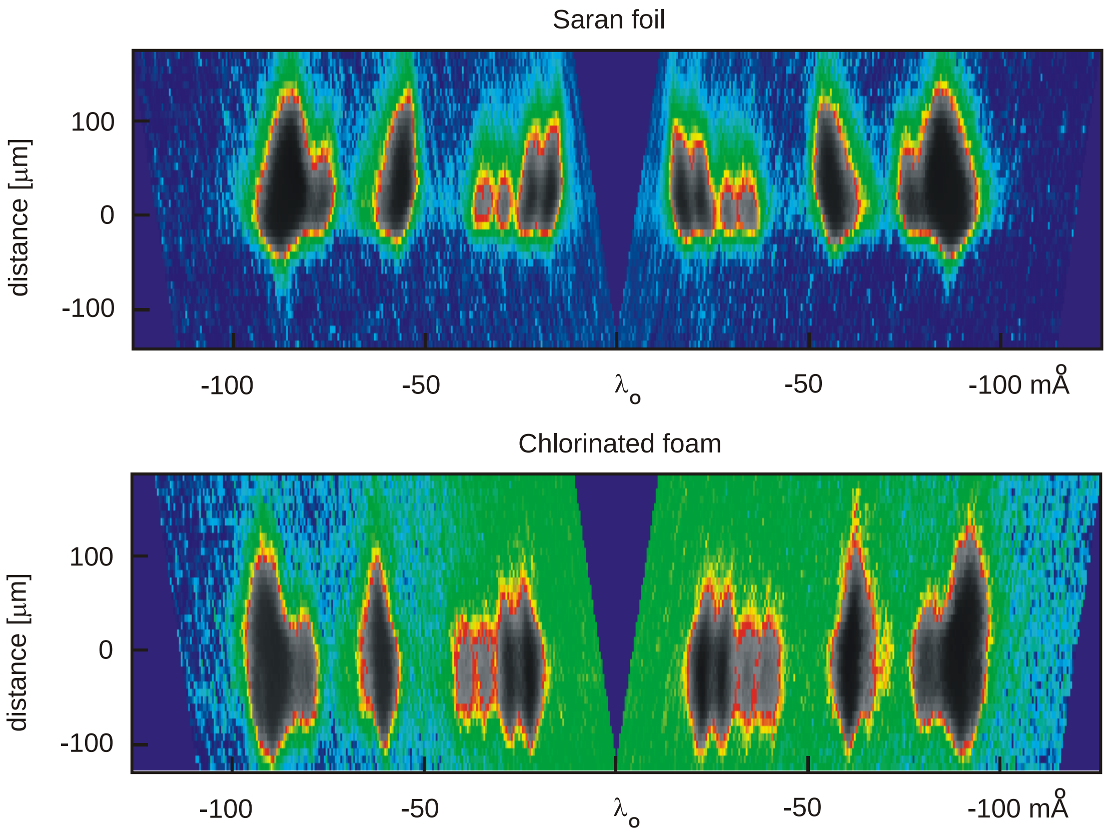

Spectra of Cl Heα group observed in 12-µm-thick saran foil ($C_2H_2Cl_2$) and TMPTA Cl-doped foam 20/25 (thickness 480 µm); angle of observation 22° to target surface, 120 J/1ω (1.315 µm), 0.4 ns, focal spot ø 80 µm (6×10^{15} W/cm^2)

Astrophysically Related Experiments

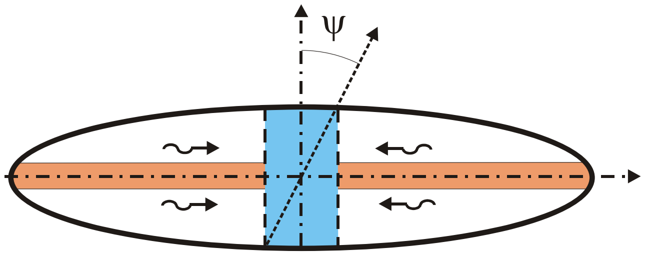

Enhancement factor defined as an intensity ratio of the optically thick and thin lines $f = I_{thick}(\psi)/I_{thin}(\psi)$

standard expectation: opacity increase can only initiate a monotonic decrease of f *Doyle J.G. et al, Mon. Not. R. Astron. Soc. 193 (1980) 947*

controversial effect predicted for stellar coronas:
f may undergo initial rise with increasing opacity before falling down
Kastner S.O. et al, Astrophys. J. 553 (2001) 421

mechanism behind enhancement – transverse radiative transfer effect:
excited states pumped by photons traversing longer (unobserved) paths

condition required for observation of this effect:
plasma slab extending to infinity in one direction, finite depth in other
coronal state (radiative deexcitation dominates the collisional one)

positive confirmation of this effect – possibility to spectroscopically derive geometric information on spatially unresolvable stellar objects
Kerr F.M. et al, JQSRT 99 (2006) 363

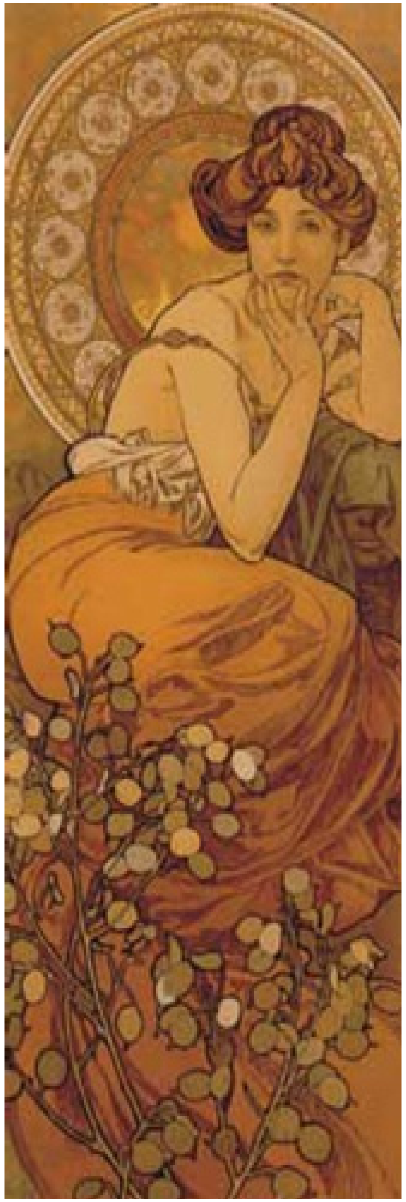

Thank You

for Your Attention!

Electron Density Evolution in TMPTA Foam

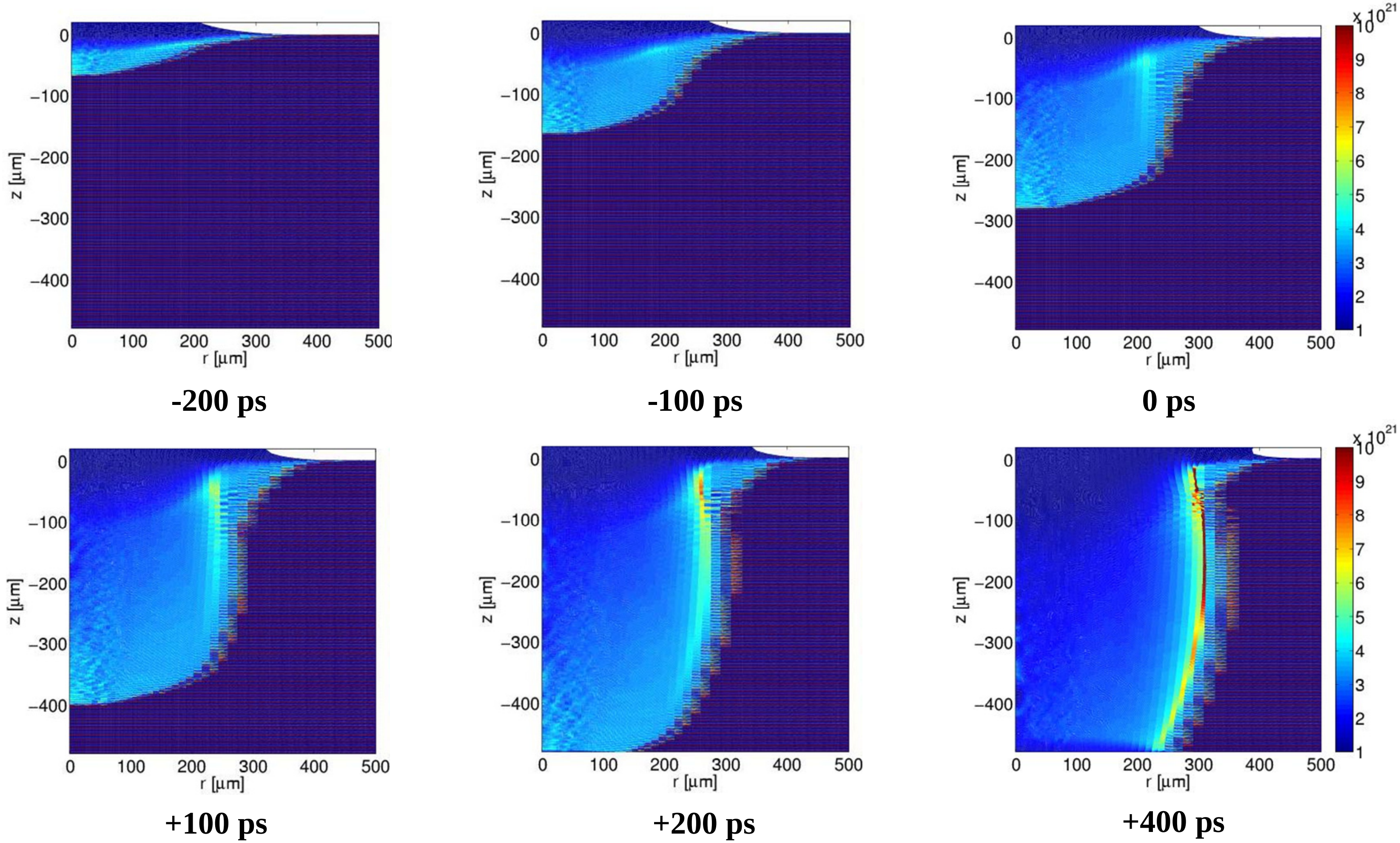

Structured foam, density 10 mg/cm^3, pore size 2 µm, foam thickness 480 µm

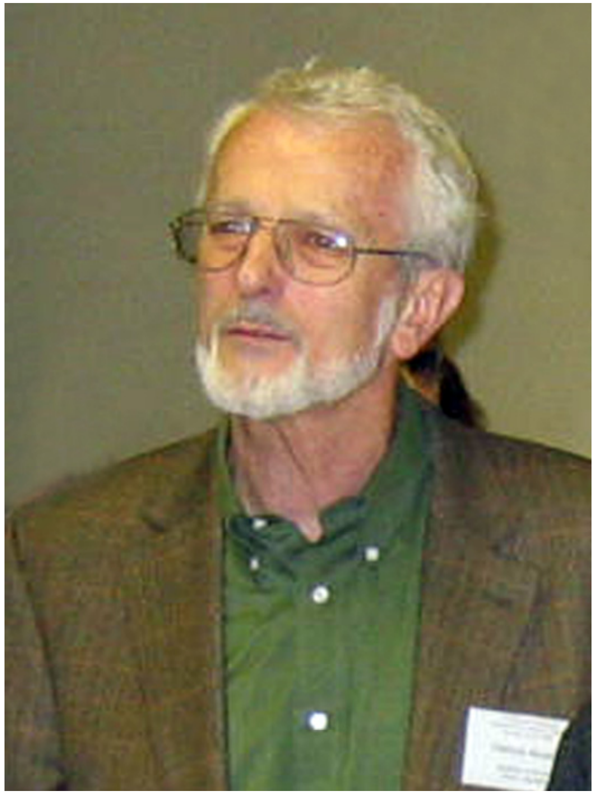

O. Renner